Digital Signal Processing 46 (2015) 32–40

Contents lists available at ScienceDirect

Digital Signal Processing

www.elsevier.com/locate/dsp

Joint magnitude and phase constrained STAP approach ☆

Jingwei Xu [a,*], Shengqi Zhu [a], Guisheng Liao [a], Lei Huang [b]

[a] National Laboratory of Radar Signal Processing, Xidian University, Xi'an 710071, China
[b] College of Information Engineering, Shenzhen University, Shenzhen 518060, China

ARTICLE INFO

Article history:
Available online 1 September 2015

Keywords:
Space–time adaptive processing
Linearly constrained minimum variance
Joint magnitude and phase constraints
Target contamination
Linear-phase response

ABSTRACT

The performance of space–time adaptive processing (STAP) radar degrades dramatically when the target occurs in the training data. Traditional robust linearly constrained minimum variance (LCMV) STAP method uses magnitude constraint to maintain the mainlobe of the STAP beamformer. In this paper, a joint magnitude and phase constrained (MPC) STAP method is proposed with the phase constraint incorporated in the response vector of the beamformer. The explicit expression of the phase constraint is derived by exploring the conjugate symmetric characteristic of the adaptive weights. With joint magnitude and phase constraints imposed on several discrete points in the mainlobe region, the MPC-STAP approach has good robustness against target contamination. In addition, the linear-phase response can be guaranteed by the proposed method, which provides distortionless response in both spatial and temporal domains. Simulation results are provided to demonstrate the effectiveness of the proposed method.

1. Introduction

Moving target indication (MTI) with airborne radar systems is an important operational mode in providing continuous surveillance of both aircraft and ground moving targets. Space–time adaptive processing (STAP) method could suppress the ground clutter and interference by combining the spatial and temporal degrees of freedom (DOFs), which has tremendous potential for improving the detection performance of airborne radar systems [1].

In conventional STAP radar, the covariance matrix of clutter and interference is usually estimated with the training data collected from ranges adjacent to the range under test. It is usually assumed that the training data satisfies the identical independent distribution (IID) condition. Under this condition, the amount of training data required for proper estimation of the covariance matrix is between 2 and 5 times the number of DOFs of the processor [2]. This is particularly challenging for STAP radar with its DOFs equal to NK (N is element number and K is pulse number), especially in nonstationary or nonhomogeneous environments [3]. To maintain the performance of STAP radar with limited sample supports, some suboptimal STAP approaches have been proposed, such as [1,4,5]. Additionally, the performance degradation of STAP radar in practice may also be caused by the range dependence of clutter. In this situation, many effective clutter compensation techniques have been presented to mitigate range-dependent clutter [6–10]. However, none of these suboptimal STAP methods and clutter compensation techniques could overcome the performance loss due to the presence of target signal in the training data. In this case, the performance of STAP radar degrades severely [11,12].

The training data corrupted by target signal, referred to as target contamination, increases the nonstationary of the clutter since the range resolution of the radar systems becomes higher [12]. Meanwhile, the need of multiple ranges to estimate the clutter covariance matrix might also cause inter-target contamination effects. This might occur when multiple close targets are presented in the received data. Since the covariance matrix is obtained by using an unsupervised training method, this will cause the covariance matrix error and the resultant performance degradation. Errors increase the influence of target contamination and/or inter-target contamination, resulting in further performance degradation of STAP radar. Generally, there are two kinds of errors. One is the covariance matrix error which is caused by small sample support of the training data whereas the other is the target steering vector error which is induced by the uncertainty of target parameter including the direction-of-arrival and Doppler frequency mismatches, imperfect array calibration error and distorted antenna shape and so on. In practice, the assumption of a rough knowledge of target parameters is reasonable, especially in target tracking situations.

☆ This work was supported by the National Natural Science Foundation of China (NSFC) (Grants 61231017 and 91438106).

* Corresponding author.
E-mail addresses: xujingwei1987@163.com (J. Xu), zhushengqi8@163.com (S. Zhu), gsliao@xidian.edu.cn (G. Liao), lhuang@szu.edu.cn (L. Huang).

http://dx.doi.org/10.1016/j.dsp.2015.08.011
1051-2004/

To overcome the performance degradation due to covariance error and steering vector error, a diagonal loading technique has been addressed in [13–15]. However, it is not clear how to choose the optimal diagonal loading factor. The target self-whitening is considered in [16–18] with a linearly constrained minimum variance (LCMV) beamforming method proposed to mitigate the signal cancellation effect. A two-point quadratically constrained beamforming approach [19] robust against DOA mismatch is proposed, which can be viewed as an LCMV processor with response vector further optimized. The phase of the response vector is optimally determined in [19]. However, it is only suitable for the two-point constrained beamforming. Recently, several robust methods with clear theoretical background have been proposed [20,21], whose diagonal loading factor can be analytically determined. The designed processors are robust against target contamination and arbitrary steering vector errors. The magnitude constrained approach which is robust against a large steering direction is derived in [22] where the magnitude response is constrained within the lower and upper bounds. It can generate an approximately flat magnitude response in the mainlobe of the beampattern, which is suitable in adaptive digital beamforming. In [22], the array output power and magnitude response are transformed into linear functions of the autocorrelation sequence of the array weight. In order to calculate the solution, a semidefinite programming based method is proposed in [23] and an iteratively robust beamforming method is presented in [24]. In [25], a phase response constrained robust beamforming method is proposed, which generates flat magnitude response and linear-phase response in the mainlobe region. It has been pointed in [26,27] that the performance of beamformer can be improved by exploiting the conjugate symmetric characteristic of the weights. To alleviate the target contamination problem in STAP radar, a robust direct data domain (DDD) approach is proposed based on worst-case optimization in [28]. This method could sufficiently improve the target detection performance. In [29], the target contamination problem is addressed based on the iterative adaptive approach by utilizing a small number of training data adjacent to the range bin under test.

In STAP radar, the target detection performance suffers degradation when only magnitude constraint is adopted. In this paper, a novel joint magnitude and phase constrained (MPC) STAP approach is proposed, where both magnitude and phase constraints are imposed on several points around the mainlobe of STAP radar. By incorporating the phase constraint in designing the STAP beamformer, the performance is improved and the robustness against target contamination is enhanced. By exploring the conjugate symmetric characteristic of the adaptive weights, the explicit expression of the phase constraint is derived, which guarantees the distortionless response of STAP radar in both spatial and temporal domains. Besides, the magnitude constraint is determined based on the criterion that the mainlobe of STAP radar approaches that of the non-adaptive processor.

The rest of this paper is organized as follows. In Section 2, the signal model is presented and the magnitude constrained STAP method is formulated. In Section 3, the novel MPC-STAP method is proposed with explicit expression of the phase constraint derived. The linear-phase response property and the robustness against target contamination are studied. In Section 4, simulation results are provided to demonstrate the effectiveness of the proposed method. The conclusions are given in Section 5.

2. Signal model and problem formulations

Without loss of generality, we consider an N-elemental half-wavelength spaced uniform linear array transmitting K coherent pulses and collecting L range bins space–time data. Assuming an arbitrary scatter of the lth range bin at direction ψ_i (measured from the axis of the array), the clutter echo of the lth range bin can be expressed as

$$\mathbf{x}_{\mathbf{c}}(l) = \sum_{i=1}^{N_c} \mathbf{c}_i(l, \psi_i, f_i) = \sum_{i=1}^{N_c} \xi_i(l)\mathbf{a}(\psi_i) \otimes \mathbf{b}(f_i) \tag{1}$$

where

- N_c stands for the number of independent scattering patches within the iso-range bin;
- $\mathbf{c}_i(l, \psi_i, f_i) \in \mathbb{C}^{NK\times 1}$ is the contribution of the ith scattering patch;
- $\xi_i(l)$ is the reflecting coefficient of the ith scattering patch of the lth range bin;
- $\otimes$ denotes the Kronecker product operator;
- $\mathbf{a}(\psi_i) \in \mathbb{C}^{N\times 1}$ and $\mathbf{b}(f_i) \in \mathbb{C}^{K\times 1}$ are respectively the spatial steering vector and temporal steering vector with ψ_i and f_i being the corresponding angle and Doppler frequency, respectively;

$$\mathbf{a}(\psi_i) = \left[1, \exp\left\{j2\pi \frac{d}{\lambda}\cos(\psi_i)\right\}, \cdots, \exp\left\{j2\pi \frac{d}{\lambda}\cos(\psi_i)(N-1)\right\}\right]^{\mathrm{T}} \tag{2}$$

$$\mathbf{b}(f_i) = \left[1, \exp\left\{j2\pi \frac{f_i}{f_{\mathrm{PRF}}}\right\}, \cdots, \exp\left\{j2\pi \frac{f_i}{f_{\mathrm{PRF}}}(K-1)\right\}\right]^{\mathrm{T}} \tag{3}$$

where the superscript $^{\mathrm{T}}$ denotes transpose operator, d is the element spacing, λ is the wavelength of radar, f_{PRF} is the pulse repetitive frequency (PRF), $f_i = 2v\cos(\psi_i)/\lambda$ is the Doppler frequency in sidelooking geometry and v is the velocity of the platform.

In order to maximize the signal-to-clutter-plus-noise ratio (SCNR), the commonly used STAP processor based on minimum variance distortionless response (MVDR) criterion is written as

$$\min_{\mathbf{w}} \mathbf{w}^{\mathrm{H}}\mathbf{R}\mathbf{w} \text{ subject to } \mathbf{w}^{\mathrm{H}}\mathbf{s}_0(\psi_0, f_0) = 1 \tag{4}$$

where the superscript $^{\mathrm{H}}$ means Hermitian transpose, $\mathbf{s}_0(\psi_0, f_0) = \mathbf{a}(\psi_0) \otimes \mathbf{b}(f_0)$ is the assumed space–time steering vector of target with ψ_0 and f_0 denoting the angle and Doppler frequency of the target, $\mathbf{R}$ is the clutter-plus-noise covariance matrix. Note that the estimated covariance matrix is commonly utilized in practice, which is written as $\hat{\mathbf{R}} = \frac{1}{L}\sum_{l=1}^{L}\mathbf{x}(l)\mathbf{x}^{\mathrm{H}}(l)$ with $\mathbf{x}(l)$ being the received snapshot consisting of target, clutter and Gaussian noise. Generally, the range under test together with several adjacent ranges (known as “guard ranges”) is excluded. However, with the increase of range resolution, a target will expand into several range bins. Thus, the training support may be corrupted by the target. The traditional MVDR STAP method is sensitive to target contamination which causes target self-whitening. Moreover, the moving targets in other range bins may have similar angles and Doppler frequencies with the desired target, which will cause inter-target contamination effect.

To enhance the robustness of the STAP radar, the LCMV beamformer [16] addresses uncertainty in the mainlobe response by using a set of unity-gain constraints in a small spread of angles and Doppler frequencies. The LCMV-STAP beamformer can be expressed as

$$\min_{\mathbf{w}} \mathbf{w}^{\mathrm{H}}\hat{\mathbf{R}}\mathbf{w} \text{ subject to } \mathbf{w}^{\mathrm{H}}\mathbf{C} = \mathbf{g}^{\mathrm{T}} \tag{5}$$

where $\mathbf{C} \in \mathbb{C}^{NK\times M}$ is the constraint matrix which contains M constraint vectors and $\mathbf{g} \in \mathbb{R}^{M\times 1}$ is the desired response vector corresponding to these points. The LCMV-STAP commonly forces

the magnitude responses of the M points to be unity, i.e. $\mathbf{g} = [1, 1, \cdots, 1]^{\mathrm{T}}$, to broaden the mainbeam of the beampattern. However, the phase constraint is left unconsidered. Actually, the phase of $\mathbf{g}$ is mismatched with the optimal space–time processor, which causes distorted response of the mainlobe in the STAP beamformer. In [22–24], magnitude constraint is considered to obtain flat magnitude response of the mainlobe, that is,

$$\min_{\mathbf{w}} \mathbf{w}^{\mathrm{H}}\hat{\mathbf{R}}\mathbf{w} \text{ subject to } b_L \le \left|\mathbf{w}^{\mathrm{H}}\mathbf{s}(\psi, f)\right| \le b_U, (\psi, f) \in \Omega \tag{6}$$

where Ω is the region of interest and b_L and b_U are the lower and upper bounds of the magnitude response in the mainlobe region. However, the magnitude constrained method in [22–24] is not suitable for STAP radar because the data structure is different from that in array digital beamforming.

3. Joint magnitude and phase constrained STAP method

In this section, we propose a novel MPC-STAP method to maintain the mainlobe of the STAP radar. In contrast with the traditional LCMV-STAP method, we exploit the complex-valued response vector and mean to generate distortionless output in both spatial and temporal domains.

In order to approach the response of the non-adaptive processor in the region of interest, we adopt a sufficient approximation technique by choosing a set of uniformly-spaced discrete points in angle-Doppler plane. By incorporating the phase constraint in the response vector, we reconsider the STAP beamformer as

$$\min_{\mathbf{w}} \mathbf{w}^{\mathrm{H}}\hat{\mathbf{R}}\mathbf{w} \text{ subject to } \mathbf{w}^{\mathrm{H}}\mathbf{C} = \mathbf{u}^{\mathrm{T}} \tag{7}$$

where $\mathbf{C}$ is the constraint matrix which is identical with that in (5) and $\mathbf{u}$ is the complex-valued response vector, that is,

$$\mathbf{u} = (\alpha_{11}\exp\{j\beta_{11}\}, \alpha_{21}\exp\{j\beta_{21}\}, \cdots, \alpha_{P1}\exp\{j\beta_{P1}\}, \cdots, \alpha_{pq}\exp\{j\beta_{pq}\}, \cdots, \alpha_{PQ}\exp\{j\beta_{PQ}\})^{\mathrm{T}} \tag{8}$$

where $\alpha_{11}, \cdots, \alpha_{PQ}$ are the magnitude constraints, $\beta_{11}, \cdots, \beta_{PQ}$ are the phase constraints and P and Q are the number of discrete points in angle and Doppler frequency dimensions, respectively. Note that the response vector $\mathbf{u}$ is different from that in the traditional LCMV-STAP beamformer since it contains the phase constraint. Fig. 1 shows the constraint points in the spatial and temporal domains. Note that the possible target is in the interested region.

Considering the complex-valued response vector, we obtain the adaptive weight by using the Lagrangian approach as [18]

$$\mathbf{w} = \hat{\mathbf{R}}^{-1}\mathbf{C}(\mathbf{C}^{\mathrm{H}}\hat{\mathbf{R}}^{-1}\mathbf{C})^{-1}\mathbf{u}^{*} \tag{9}$$

where the superscript asterisk indicates complex conjugate. The STAP response is desired to be distortionless in both spatial and temporal domains. The distortionless response is of critical importance in interferometric phase estimation and angle and Doppler estimation. Although there are many works developed concerning the magnitude constraint [16–19,22–24], the phase constraint is left unconsidered. In the following, we present the explicit expression of the phase constraint in order to implement distortionless response in the mainlobe. Moreover, the robustness against target contamination of the MPC-STAP approach is justified.

3.1. Linear-phase response

As we know, the frequency response of a length-N finite impulse response (FIR) filter is a linear function of the frequency when we consider the FIR filter with symmetric impulse response [30,31]. In STAP radar, when the adaptive weight is conjugated

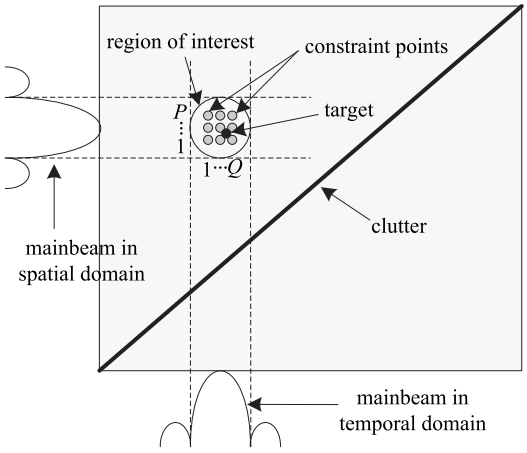

Fig. 1. Sketch of constraint points in spatial and temporal domains.

symmetric, the response of the STAP beamformer is a linear function of angle and Doppler frequency. Thus, in order to obtain linear-phase response, additional constraints should be imposed on the adaptive weights, that is,

$$\min_{\mathbf{w}} \mathbf{w}^{\mathrm{H}}\hat{\mathbf{R}}\mathbf{w} \text{ subject to } \begin{cases} \mathbf{w}^{\mathrm{H}}\mathbf{C} = \mathbf{u}^{\mathrm{T}} \\ \mathbf{w} = (\mathbf{J}_s \otimes \mathbf{J}_t)\mathbf{w}^{*} = \mathbf{J}\mathbf{w}^{*} \end{cases} \tag{10}$$

where $\mathbf{J}_s$, $\mathbf{J}_t$ and $\mathbf{J}$ are transposition matrices in element dimension, pulse dimension and element–pulse dimension, respectively, i.e.,

$$\mathbf{J}_s = \begin{pmatrix} 0 & & 1 \\ & \iddots & \\ 1 & & 0 \end{pmatrix}_{N\times N}, \quad \mathbf{J}_t = \begin{pmatrix} 0 & & 1 \\ & \iddots & \\ 1 & & 0 \end{pmatrix}_{K\times K},$$

$$\mathbf{J} = \mathbf{J}_s \otimes \mathbf{J}_t = \begin{pmatrix} 0 & & 1 \\ & \iddots & \\ 1 & & 0 \end{pmatrix}_{NK\times NK} \tag{11}$$

In [26,27], this conjugate symmetric constraint is utilized to improve the performance and computation efficiency. In this work, we transform the conjugate symmetric constraints into the desired phase constraint of the response vector. Without loss of generality, we choose the first element and first pulse as reference. Thus, we obtain

$$\mathbf{C} = \tilde{\mathbf{C}}\boldsymbol{\Phi} \tag{12}$$

where

$$\tilde{\mathbf{C}} = (\tilde{\mathbf{c}}_1, \cdots, \tilde{\mathbf{c}}_{PQ}) \tag{13}$$

$$\begin{aligned} \tilde{\mathbf{c}}(\psi, f) = &\left[\exp\left\{-j2\pi\frac{d}{\lambda}\cos(\psi)\frac{N-1}{2}\right\}, \right. \\ &\exp\left\{-j2\pi\frac{d}{\lambda}\cos(\psi)\frac{N-3}{2}\right\}, \cdots, \\ &\left.\exp\left\{j2\pi\frac{d}{\lambda}\cos(\psi)\frac{N-1}{2}\right\}\right]^{\mathrm{T}} \\ \otimes &\left[\exp\left\{-j2\pi\frac{f}{f_{\mathrm{PRF}}}\frac{K-1}{2}\right\}, \right. \\ &\exp\left\{-j2\pi\frac{f}{f_{\mathrm{PRF}}}\frac{K-3}{2}\right\}, \cdots, \\ &\left.\exp\left\{j2\pi\frac{f}{f_{\mathrm{PRF}}}\frac{K-1}{2}\right\}\right]^{\mathrm{T}} \end{aligned} \tag{14}$$

$$\boldsymbol{\Phi} = \mathrm{diag}\left\{\exp\left\{j2\pi\left(\frac{N-1}{2}\frac{d}{\lambda}\cos(\psi_1)+\frac{K-1}{2}\frac{f_1}{f_{\mathrm{PRF}}}\right)\right\},\cdots,\right.$$
$$\left.\exp\left\{j2\pi\left(\frac{N-1}{2}\frac{d}{\lambda}\cos(\psi_{PQ})+\frac{K-1}{2}\frac{f_{PQ}}{f_{\mathrm{PRF}}}\right)\right\}\right\} \quad (15)$$

Note that $\tilde{\mathbf{C}} = \mathbf{J}\tilde{\mathbf{C}}^*$. The problem in (7) can be rewritten as

$$\min_{\mathbf{w}} \mathbf{w}^{\mathrm{H}}\hat{\mathbf{R}}\mathbf{w} \text{ subject to } \mathbf{w}^{\mathrm{H}}\mathbf{C} = \mathbf{w}^{\mathrm{H}}\tilde{\mathbf{C}}\boldsymbol{\Phi} = \mathbf{u}^{\mathrm{T}} \quad (16)$$

The adaptive weight is expressed as

$$\mathbf{w} = \hat{\mathbf{R}}^{-1}(\tilde{\mathbf{C}}\boldsymbol{\Phi})\left[\left(\tilde{\mathbf{C}}\boldsymbol{\Phi}\right)^{\mathrm{H}}\hat{\mathbf{R}}^{-1}\left(\tilde{\mathbf{C}}\boldsymbol{\Phi}\right)\right]^{-1}\mathbf{u}^*$$
$$= \hat{\mathbf{R}}^{-1}\tilde{\mathbf{C}}\left(\tilde{\mathbf{C}}^{\mathrm{H}}\hat{\mathbf{R}}^{-1}\tilde{\mathbf{C}}\right)^{-1}\boldsymbol{\Phi}\mathbf{u}^* \quad (17)$$

where $\boldsymbol{\Phi}^* = \boldsymbol{\Phi}^{-1}$. Since $\hat{\mathbf{R}}$ is Hermitian symmetric matrix, i.e., $\hat{\mathbf{R}} = \hat{\mathbf{R}}^{\mathrm{H}}$, we obtain

$$\mathbf{J}\mathbf{w}^* = \mathbf{J}\left[\hat{\mathbf{R}}^{-1}\tilde{\mathbf{C}}\left(\tilde{\mathbf{C}}\hat{\mathbf{R}}^{-1}\tilde{\mathbf{C}}\right)^{-1}\boldsymbol{\Phi}\mathbf{u}^*\right]^*$$
$$= \mathbf{J}\left(\hat{\mathbf{R}}^*\right)^{-1}\tilde{\mathbf{C}}^*\left[(\tilde{\mathbf{C}}^*)^{\mathrm{H}}(\hat{\mathbf{R}}^*)^{-1}\tilde{\mathbf{C}}^*\right]^{-1}\boldsymbol{\Phi}^*\mathbf{u}$$
$$= \mathbf{J}(\hat{\mathbf{R}}^*)^{-1}\mathbf{J}\tilde{\mathbf{C}}\left[(\mathbf{J}\tilde{\mathbf{C}})^{\mathrm{H}}(\hat{\mathbf{R}}^*)^{-1}\mathbf{J}\tilde{\mathbf{C}}\right]^{-1}\boldsymbol{\Phi}^*\mathbf{u}$$
$$= (\mathbf{J}\hat{\mathbf{R}}^*\mathbf{J})^{-1}\tilde{\mathbf{C}}\left(\tilde{\mathbf{C}}^{\mathrm{H}}(\mathbf{J}\hat{\mathbf{R}}^*\mathbf{J})^{-1}\tilde{\mathbf{C}}\right)^{-1}\boldsymbol{\Phi}^*\mathbf{u}$$
$$= \hat{\mathbf{R}}^{-1}\tilde{\mathbf{C}}\left(\tilde{\mathbf{C}}^{\mathrm{H}}\hat{\mathbf{R}}^{-1}\tilde{\mathbf{C}}\right)^{-1}\boldsymbol{\Phi}^*\mathbf{u} \quad (18)$$

It is observed that $\mathbf{w} = \mathbf{J}\mathbf{w}^*$ is satisfied if and only if

$$\boldsymbol{\Phi}\mathbf{u}^* = \boldsymbol{\Phi}^*\mathbf{u} \quad (19)$$

Therefore, the element in vector $\boldsymbol{\Phi}\mathbf{u}^*$ is real-valued, leading to

$$\beta_{pq} = 2\pi\left(\frac{N-1}{2}\frac{d}{\lambda}\cos(\psi_p)+\frac{K-1}{2}\frac{f_q}{f_{\mathrm{PRF}}}\right),$$
$$p = 1,\cdots,P; q = 1,\cdots,Q \quad (20)$$

Equation (20) is the explicit expression of the phase constraint in the response vector $\mathbf{u}$ in order to obtain linear-phase response with respect to angle and Doppler frequency. In other words, if the phase of response vector $\mathbf{u}$ is chosen as (20), the conjugate symmetric weight constraint can always be satisfied. Thus, the linear-phase response of the STAP radar can be guaranteed. Comparing the proposed MPC-STAP beamformer using phase constraint as (20) with the beamformer in (10), we can see that the proposed approach uses fewer DOFs. The number of constraints in (10) is $\frac{NK}{2} + PQ$ while the number of constraints in the proposed approach is reduced to PQ. By incorporating and properly settling the phase constraint, the STAP beamformer can provide distortionless response in both spatial and temporal domains.

The linear-phase response in separated domain is required in some scenarios, which can be obtained by using the aforementioned method in spatial or temporal domain. Here, we take the case in temporal domain as an example. The problem can be expressed as

$$\min_{\mathbf{w}} \mathbf{w}^{\mathrm{H}}\hat{\mathbf{R}}\mathbf{w} \text{ subject to } \begin{cases}\mathbf{w}^{\mathrm{H}}\mathbf{C} = \mathbf{u}^{\mathrm{T}} \\ \mathbf{w} = (\mathbf{I}\otimes\mathbf{J}_t)\mathbf{w}^*\end{cases} \quad (21)$$

where the adaptive weight is conjugate symmetric in temporal domain. The adaptive weight is written as

$$\mathbf{w} = \hat{\mathbf{R}}^{-1}(\bar{\mathbf{C}}\bar{\boldsymbol{\Phi}})\left[\left(\bar{\mathbf{C}}\bar{\boldsymbol{\Phi}}\right)^{\mathrm{H}}\hat{\mathbf{R}}^{-1}\left(\bar{\mathbf{C}}\bar{\boldsymbol{\Phi}}\right)\right]^{-1}\mathbf{u}^*$$
$$= \hat{\mathbf{R}}^{-1}\bar{\mathbf{C}}\left(\bar{\mathbf{C}}^{\mathrm{H}}\hat{\mathbf{R}}^{-1}\bar{\mathbf{C}}\right)^{-1}\bar{\boldsymbol{\Phi}}\mathbf{u}^* \quad (22)$$

where $\bar{\mathbf{C}} = (\mathbf{I}\otimes\mathbf{J}_t)\bar{\mathbf{C}}^*$, $\bar{\boldsymbol{\Phi}} = \mathrm{diag}\{\exp\{j2\pi\frac{K-1}{2}\frac{f_1}{f_{\mathrm{PRF}}}\},\cdots,\exp\{j2\pi\times\frac{K-1}{2}\frac{f_{PQ}}{f_{\mathrm{PRF}}}\}\}$. The covariance matrix is also conjugate symmetric in this case, i.e., $\mathbf{R} = (\mathbf{I}\otimes\mathbf{J}_t)\hat{\mathbf{R}}^*(\mathbf{I}\otimes\mathbf{J}_t)$. Thus, $\mathbf{w} = (\mathbf{I}\otimes\mathbf{J}_t)\mathbf{w}^*$ is satisfied if and only if these elements in $\bar{\boldsymbol{\Phi}}\mathbf{u}^*$ are real-valued, i.e.,

$$\beta_{pq} = 2\pi\frac{K-1}{2}\frac{f_q}{f_{\mathrm{PRF}}}, \quad p = 1,\cdots,P; q = 1,\cdots,Q \quad (23)$$

Therefore, the resulted STAP beamformer is distortionless in temporal domain. Similarly, the proposed method is applicable in spatial domain and the phase constraint is written as

$$\beta_{pq} = 2\pi\frac{N-1}{2}\frac{d}{\lambda}\cos(\psi_p), \quad p = 1,\cdots,P; q = 1,\cdots,Q \quad (24)$$

As to the magnitude constraint in the response vector, in order to approaching the magnitude response of the non-adaptive space–time processor, the magnitude constraint is settled as

$$\alpha_{pq} = \left|\mathbf{s}_0^{\mathrm{H}}(\psi_0, f_0)\mathbf{s}(\psi_p, f_q)\right|, \quad p = 1,\cdots,P; q = 1,\cdots,Q \quad (25)$$

Note that ψ_0 and f_0 are the estimated angle and Doppler frequency of the target. As we have mentioned that the angle and Doppler frequency are a rough knowledge of target parameters in practice.

3.2. Robustness against target contamination

By incorporating the phase constraint, the MPC-STAP approach can provide good robustness against target contamination. The SCNR loss factor is commonly used to assess the detection performance of STAP radar. It is defined as the ratio of clutter-limited output SCNR to the noise-limited output signal-to-noise ratio (SNR):

$$\mathrm{SCNR}_{\mathrm{loss}} = \frac{\mathrm{SCNR}_{\mathrm{out}}}{\mathrm{SNR}_{\mathrm{out}}} = \frac{\frac{\mathbf{w}^{\mathrm{H}}\mathbf{R}_{\mathbf{s}}\mathbf{w}}{\mathbf{w}^{\mathrm{H}}\mathbf{R}_{\mathbf{c+n}}\mathbf{w}}}{\frac{\mathbf{w}^{\mathrm{H}}\mathbf{R}_{\mathbf{s}}\mathbf{w}}{\mathbf{w}^{\mathrm{H}}\mathbf{R}_{\mathbf{n}}\mathbf{w}}} = \frac{\mathbf{w}^{\mathrm{H}}\mathbf{R}_{\mathbf{s}}\mathbf{w}}{\mathbf{w}^{\mathrm{H}}\mathbf{R}_{\mathbf{c+n}}\mathbf{w}}\frac{\sigma_n^2}{\sigma_s^2 NK} \quad (26)$$

where $\mathbf{R}_{\mathbf{s}}$, $\mathbf{R}_{\mathbf{c+n}}$ and $\mathbf{R}_{\mathbf{n}}$ are the signal covariance matrix, clutter-plus-noise covariance matrix and noise covariance matrix, respectively, σ_s^2 and σ_n^2 are the signal and noise power, respectively. Considering the point-target case, the signal covariance matrix can be written as $\mathbf{R}_{\mathbf{s}} = \sigma_s^2\mathbf{s}_0\mathbf{s}_0^{\mathrm{H}}$. Substituting the adaptive weight (9) into (26) yields

$$\mathrm{SCNR}_{\mathrm{loss}} = \frac{\sigma_n^2}{NK}\frac{\left|\mathbf{u}^{\mathrm{T}}\left(\mathbf{C}^{\mathrm{H}}\hat{\mathbf{R}}^{-1}\mathbf{C}\right)^{-1}\mathbf{C}^{\mathrm{H}}\hat{\mathbf{R}}^{-1}\mathbf{s}_0\right|^2}{\mathbf{u}^{\mathrm{T}}\left(\mathbf{C}^{\mathrm{H}}\hat{\mathbf{R}}^{-1}\mathbf{C}\right)^{-1}\mathbf{C}^{\mathrm{H}}\hat{\mathbf{R}}^{-1}\mathbf{R}_{\mathbf{c+n}}\hat{\mathbf{R}}^{-1}\mathbf{C}\left(\mathbf{C}^{\mathrm{H}}\hat{\mathbf{R}}^{-1}\mathbf{C}\right)^{-1}\mathbf{u}^*} \quad (27)$$

Considering the target contamination, i.e., $\hat{\mathbf{R}} = \mathbf{R}_{\mathbf{c+n}} + \mathbf{R}_{\mathbf{s}}$, we obtain

$$\mathrm{SCNR}_{\mathrm{loss}} > \frac{\sigma_n^2}{NK}\frac{\left|\mathbf{u}^{\mathrm{T}}\left(\mathbf{C}^{\mathrm{H}}\hat{\mathbf{R}}^{-1}\mathbf{C}\right)^{-1}\mathbf{C}^{\mathrm{H}}\hat{\mathbf{R}}^{-1}\mathbf{s}_0\right|^2}{\mathbf{u}^{\mathrm{T}}\left(\mathbf{C}^{\mathrm{H}}\hat{\mathbf{R}}^{-1}\mathbf{C}\right)^{-1}\mathbf{C}^{\mathrm{H}}\hat{\mathbf{R}}^{-1}\hat{\mathbf{R}}\hat{\mathbf{R}}^{-1}\mathbf{C}\left(\mathbf{C}^{\mathrm{H}}\hat{\mathbf{R}}^{-1}\mathbf{C}\right)^{-1}\mathbf{u}^*}$$
$$= \frac{\sigma_n^2}{NK}\frac{\left|\mathbf{u}^{\mathrm{T}}\left(\mathbf{C}^{\mathrm{H}}\hat{\mathbf{R}}^{-1}\mathbf{C}\right)^{-1}\mathbf{C}^{\mathrm{H}}\hat{\mathbf{R}}^{-1}\mathbf{s}_0\right|^2}{\mathbf{u}^{\mathrm{T}}\left(\mathbf{C}^{\mathrm{H}}\hat{\mathbf{R}}^{-1}\mathbf{C}\right)^{-1}\mathbf{u}^*} \quad (28)$$

Define $\mathbf{P} = (\mathbf{C}^{\mathrm{H}}\hat{\mathbf{R}}^{-1}\mathbf{C})^{-1}$, $\mathbf{u}_0 = \mathbf{C}^{\mathrm{H}}\hat{\mathbf{R}}^{-1}\mathbf{s}_0$ and $\mathbf{Q} = \mathbf{P}\mathbf{u}_0\mathbf{u}_0^{\mathrm{H}}\mathbf{P}$, yielding

$$g(\mathbf{u}) = \frac{\left|\mathbf{u}^{\mathrm{T}}\left(\mathbf{C}^{\mathrm{H}}\hat{\mathbf{R}}^{-1}\mathbf{C}\right)^{-1}\mathbf{C}^{\mathrm{H}}\hat{\mathbf{R}}^{-1}\mathbf{s}_0\right|^2}{\mathbf{u}^{\mathrm{T}}\left(\mathbf{C}^{\mathrm{H}}\hat{\mathbf{R}}^{-1}\mathbf{C}\right)^{-1}\mathbf{u}^*} = \frac{\mathbf{u}^{\mathrm{T}}\mathbf{P}\mathbf{u}_0\mathbf{u}_0^{\mathrm{H}}\mathbf{P}\mathbf{u}^*}{\mathbf{u}^{\mathrm{T}}\mathbf{P}\mathbf{u}^*} = \frac{\mathbf{u}^{\mathrm{T}}\mathbf{Q}\mathbf{u}^*}{\mathbf{u}^{\mathrm{T}}\mathbf{P}\mathbf{u}^*} \tag{29}$$

Recalling the Rayleigh quotient [32], we know that $g(\mathbf{u})$ is lower and upper bounded. Note that $\mathrm{rank}(\mathbf{Q}) = 1$, the maximum value of $g(\mathbf{u})$ is achieved when $\mathbf{u}$ satisfies $\mathbf{Q}\mathbf{u} = \lambda\mathbf{P}\mathbf{u}$. We differentiate $g(\mathbf{u})$ with respect to $\mathbf{u}$ and set the derivative equal to zero. Thus, we obtain

$$\mathbf{u}^{\mathrm{T}}\mathbf{P}\mathbf{u}^*\mathbf{P}\mathbf{u}_0^*\mathbf{u}_0^{\mathrm{T}}\mathbf{P}\mathbf{u}^* - \mathbf{u}^{\mathrm{T}}\mathbf{P}\mathbf{u}_0^*\mathbf{u}_0^{\mathrm{T}}\mathbf{P}\mathbf{u}^*\mathbf{P}\mathbf{u}^* = 0 \tag{30}$$

Obviously, (30) holds when $\mathbf{u} = \mathbf{u}_0$. It should also be noted that the maximum value of (27) will not change when an additive phase term is added to $\mathbf{u}$. The inverse of the covariance matrix can be written as

$$\hat{\mathbf{R}}^{-1} = \left(\mathbf{R}_{\mathbf{c}+\mathbf{n}} + \sigma_s^2\mathbf{s}_0\mathbf{s}_0^{\mathrm{H}}\right)^{-1} = \mathbf{R}_{\mathbf{c}+\mathbf{n}}^{-1} - \frac{\sigma_s^2\mathbf{R}_{\mathbf{c}+\mathbf{n}}^{-1}\mathbf{s}_0\mathbf{s}_0^{\mathrm{H}}\mathbf{R}_{\mathbf{c}+\mathbf{n}}^{-1}}{1+\sigma_s^2\mathbf{s}_0^{\mathrm{H}}\mathbf{R}_{\mathbf{c}+\mathbf{n}}^{-1}\mathbf{s}_0} \tag{31}$$

Thus, the response vector can be expressed as

$$\mathbf{u} = \mathbf{u}_0 = \mathbf{C}^{\mathrm{H}}\left(\mathbf{R}_{\mathbf{c}+\mathbf{n}}^{-1} - \frac{\sigma_s^2\mathbf{R}_{\mathbf{c}+\mathbf{n}}^{-1}\mathbf{s}_0\mathbf{s}_0^{\mathrm{H}}\mathbf{R}_{\mathbf{c}+\mathbf{n}}^{-1}}{1+\sigma_s^2\mathbf{s}_0^{\mathrm{H}}\mathbf{R}_{\mathbf{c}+\mathbf{n}}^{-1}\mathbf{s}_0}\right)\mathbf{s}_0 = \frac{\mathbf{C}^{\mathrm{H}}\mathbf{R}_{\mathbf{c}+\mathbf{n}}^{-1}\mathbf{s}_0}{1+\sigma_s^2\mathbf{s}_0^{\mathrm{H}}\mathbf{R}_{\mathbf{c}+\mathbf{n}}^{-1}\mathbf{s}_0} \tag{32}$$

When the target is far from the clutter ridge in the spatial and temporal domains, it is reasonable to assume that the subspaces of target and clutter are orthogonal. In this case, the response vector can be approximately written as

$$\mathbf{u} \approx \frac{\mathbf{C}^{\mathrm{H}}\mathbf{s}_0}{1+\sigma_s^2\left\|\mathbf{s}_0\right\|_2^2} \tag{33}$$

The phase of the pq-th entry of $\mathbf{u}$ can be written as

$$\begin{aligned}\angle\left\{\mathbf{u}_{pq}\right\} &= \angle\left\{\mathbf{c}^{\mathrm{H}}(\psi_p, f_q)\mathbf{s}_0(\psi_0, f_0)\right\} \\ &= \pi(N-1)\frac{d}{\lambda}\left(\cos(\psi_p) - \cos(\psi_0)\right) \\ &\quad + \pi(K-1)\left(\frac{f_q}{f_{\mathrm{PRF}}} - \frac{f_0}{f_{\mathrm{PRF}}}\right)\end{aligned} \tag{34}$$

This is the phase constraint in (20) which is attached with an additive phase $-\pi(N-1)\frac{d}{\lambda}\cos(\psi_0) - \pi(K-1)\frac{f_0}{f_{\mathrm{PRF}}}$. Therefore, the SCNR loss is maximized by incorporating the phase constraint, which maintains the performance of STAP radar in the target contamination scenario.

4. Simulation results

In this section, simulation experiments are conducted to demonstrate the effectiveness of the proposed method. The simulation parameters are listed in Table 1.

4.1. Magnitude response of STAP radar comparison

In this subsection, a set of experiments is carried out and the target signal occurs in the training data. The maximum unambiguous velocity of the target in this example is 120 m/s. There will be a series of temporal steering vectors assumed to cover the whole Doppler range. In this example, the number of Doppler cells is 24 and the velocity corresponding to each Doppler cell is

$$v_m = \frac{2v_u}{24}m - v_u = v_u\left(\frac{m}{12} - 1\right), \quad m = 0, 1, \cdots, 23 \tag{35}$$

Table 1
Parameters of radar system.

Parameter	Value	Parameter	Value
Wavelength	0.32 m	Element number	12
Element spacing	0.16 m	Pulse number	12
Platform height	6000 m	PRF	1.5 kHz
Platform velocity	120 m/s	Range of interest	30 km
Looking angle	90°	CNR	60 dB

where $v_u = 120$ m/s and the subscript m indicates the mth Doppler cell. In this example, the velocity and angle of the assumed target are 30 m/s ($m = 15$) and 90° (looking angle), respectively, while the actual target is from 92° and its radial velocity equals 32 m/s. The signal-to-noise ratio (SNR) is 20 dB and the snapshot number is 200. Other parameters can be found in Table 1.

Fig. 2 shows the magnitude response of the STAP radar in spatial and temporal domains. The pentagrams in these figures denote the position of the actual target. As the training data is corrupted by the target signal, the target is treated as interference by the traditional MVDR-STAP processor, which causes target self-whitening. The traditional LCMV-STAP method is robust against target contamination by imposing several magnitude constraints around the assumed point in angle-Doppler plane. As analyzed in Section 3, nine constraint points have been used in the mainlobe region. However, it is seen that the sidelobe of LCMV-STAP method is high, which would cause performance degradation. Besides, the LCMV-STAP method would induce high noise output and be susceptible to unknown interference due to high sidelobe [33]. Fig. 2(c) plots the magnitude response of the robust STAP method based on magnitude constraint in [22]. It is seen that the method in [22] is not suitable for STAP radar. The clutter cannot be sufficiently suppressed and the performance of STAP radar suffers. By using joint magnitude and phase constraints in the mainlobe, the magnitude response of the proposed MPC-STAP method is almost impervious to target as shown in Fig. 2(d). Therefore, the target-whitening effect is avoided and the performance degradation can be mitigated.

4.2. Phase response of STAP radar comparison

The phase responses in spatial and temporal domains of the MVDR-STAP method, traditional LCMV-STAP method, magnitude constrained method in [22] and proposed MPC-STAP method are plotted in Fig. 3. The corresponding phase responses in separated spatial or temporal domain around the mainlobe of these methods are depicted in Fig. 4. Because of the target self-whitening effect of the MVDR-STAP method, its linear region in the mainlobe is reduced. As shown in Fig. 3(a) and Fig. 4, the linear-phase response of the MVDR-STAP method in spatial domain is severely destroyed. The phase response of the traditional LCMV-STAP is shown in Fig. 3(b) and Fig. 4. It is seen that the phase response is nearly flat around the mainlobe, which destroys the distortionless response of the mainlobe. For the magnitude constrained STAP method as shown in Fig. 3(c), the linear-phase response cannot be guaranteed. In contrast, the linear-phase response of the proposed MPC-STAP method in spatial and temporal domains is well maintained, as shown in Fig. 3(c) and Fig. 4. As mentioned in Section 3, the adaptive weights of the proposed method are complex symmetric, which guarantees the linear-phase response.

4.3. SCNR loss performance comparison

Fig. 5 shows the SCNR loss versus the input SNR. In low SNR region, the target signal is buried in noise and it cannot cause target self-whitening even when it occurs in the training data.

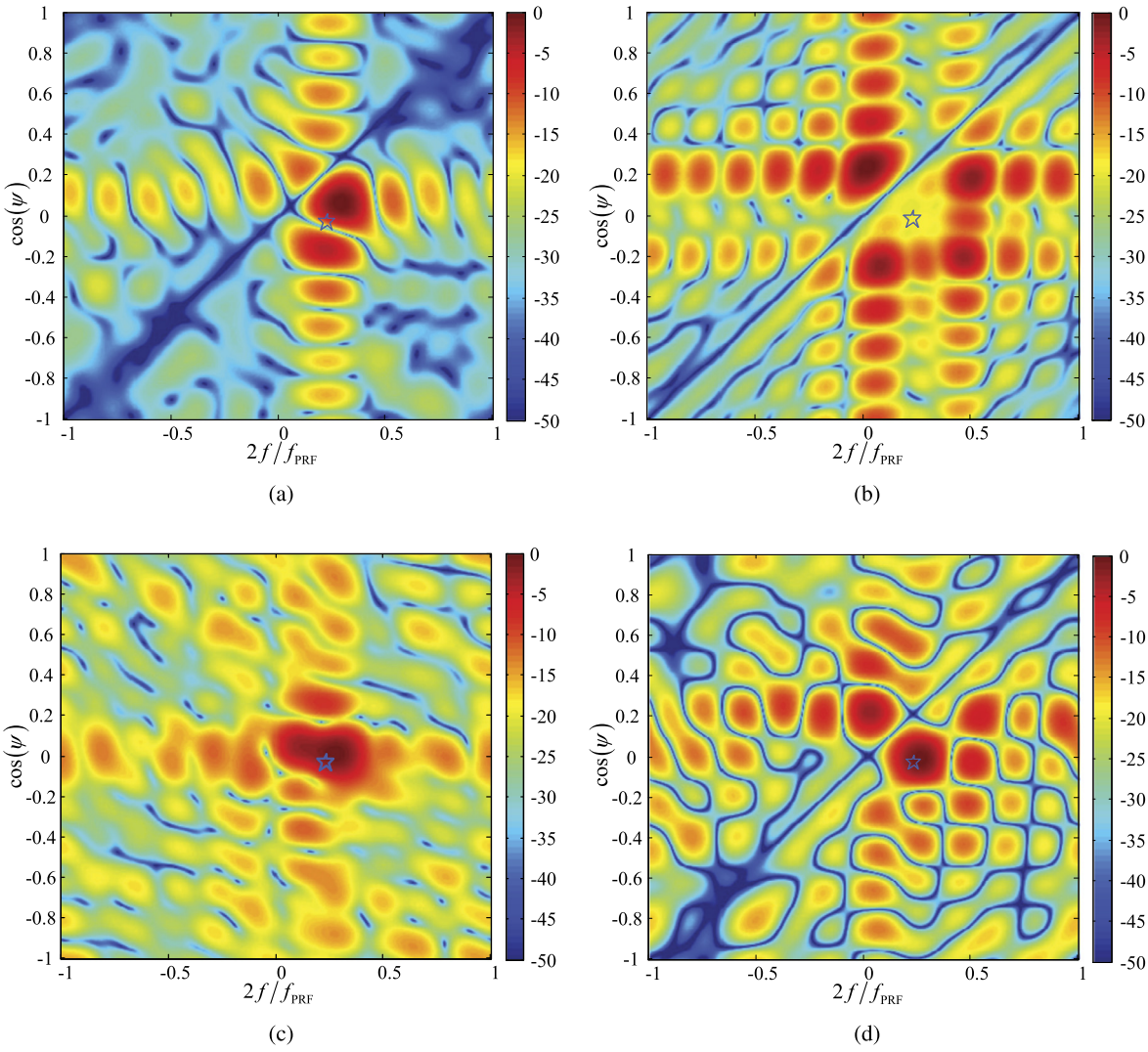

Fig. 2. Magnitude response of STAP methods in spatial and temporal domains under target contamination. (a) MVDR-STAP method, (b) LCMV-STAP method, (c) magnitude constrained STAP method [22] and (d) MPC-STAP method.

In this case, the performance of MVDR-STAP method is perfectly maintained. However, with the increase of SNR, the performance of MVDR-STAP method degrades gradually. The reason is that the MVDR-STAP method misinterprets the target as interference and tries to suppress it. In contrast, the proposed MPC-STAP method can effectively overcome the target self-whitening problem. In low SNR region, the performance of the proposed method is slightly lower (about 3 dB lower than that of MVDR-STAP method), which is induced by the DOFs consumption due to multiple constraints. In high SNR region, the MPC-STAP method is robust against the target contamination and outperforms the MVDR-STAP method. As a comparison, the empirical results of the traditional LCMV-STAP method, magnitude constrained STAP method and worst-case STAP method are provided. As the phase constraint is unconsidered in the traditional LCMV-STAP method, its performance degrades substantially though the SCNR loss is approximately invariant with the input SNR. Moreover, the magnitude constrained STAP method cannot suppress the clutter effectively and suffers severe performance degradation.

As mentioned earlier, the Doppler range is divided into 24 segments and each segment covers $\frac{1}{24}$ of the total unambiguous velocity. Similarly, the spatial frequency can also be divided into 24 segments and the beam is discretely steered to each corresponding direction. Fig. 6 gives the SCNR loss performance comparison of the traditional MVDR-STAP, the LCMV-STAP, the MPC-STAP, the worst-case optimization based STAP methods [21]. The SCNR loss curves are shown with either temporal steering vector error (Figs. 6(a) and (c)) or spatial steering vector error (Figs. 6(b) and (d)). For Figs. 6(a) and (b), we fix the input SNR at 20 dB and vary the velocity and angle errors. The velocity error is between -5 m/s and 5 m/s, while the angle error is between $-3.8°$ and $3.8°$. For Figs. 6(c) and (d), we vary the input SNR from -10 dB to 30 dB and fix the velocity error and angel error at 3 m/s and $2°$, respectively. The performance of the proposed method keeps approximately unchanged as illustrated in Figs. 6(a) and (b). The performance of the worst-case STAP method degrades when the velocity or angle error becomes larger, though its performance outperforms other methods with small errors. The performance of the MVDR-STAP method degrades dramatically even for a small mismatch between the assumed and actual targets. Furthermore, the performance loss of the traditional LCMV-STAP method is out of acceptable. It can be seen from Figs. 6(c) and (d) that the proposed method is more robust against input SNR.

By incorporating the phase constraint in the response vector, the mainlobe of the STAP beamformer can be well maintained. However, when the Doppler frequency of the assumed target is approaching that of the clutter ridge, the minimization of the total output power will conflict with the constraint condition, thus

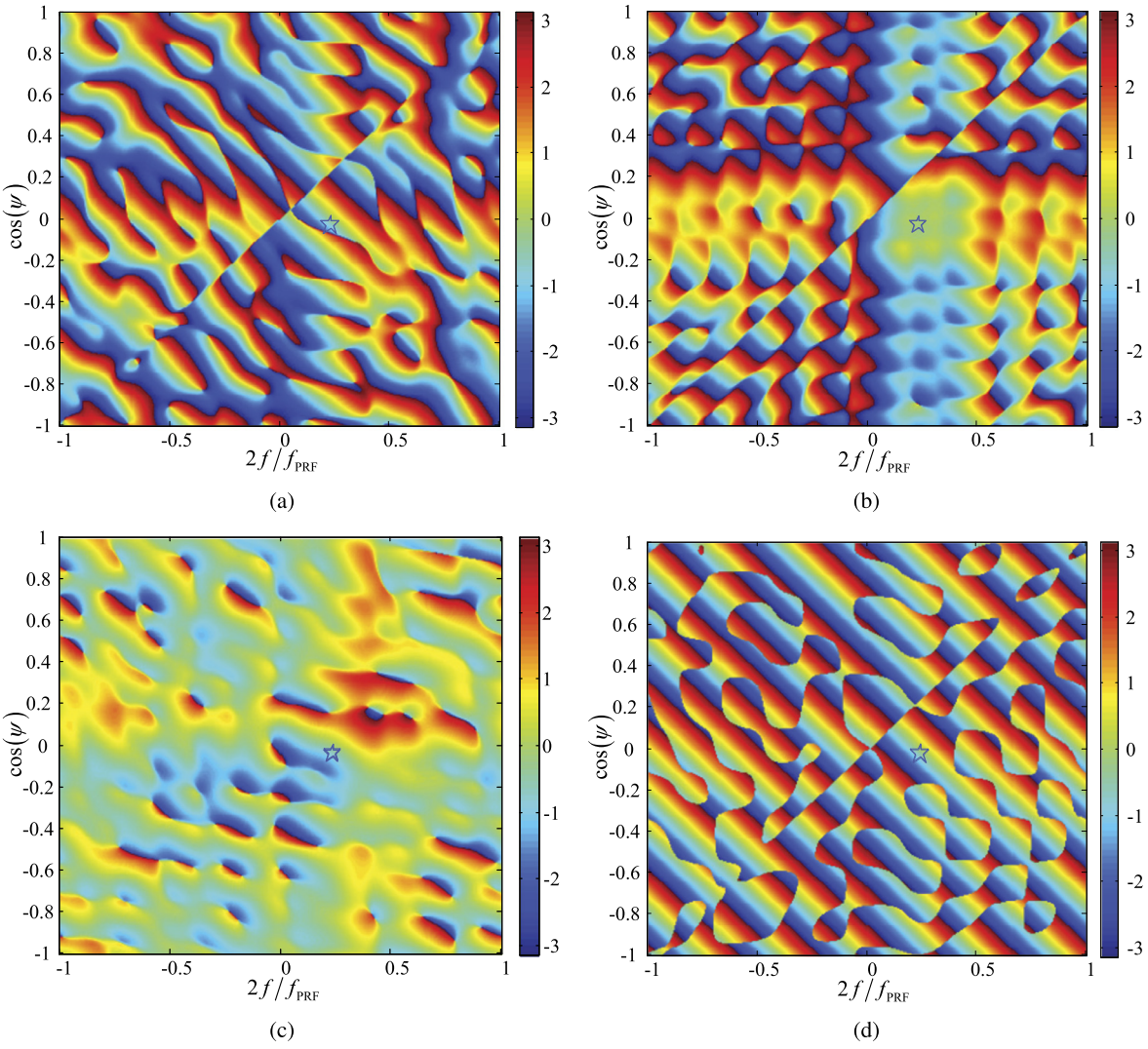

Fig. 3. Phase response of STAP methods in spatial and temporal domains under target contamination. (a) MVDR-STAP method, (b) LCMV-STAP method, (c) magnitude constrained STAP method [22] and (d) MPC-STAP method.

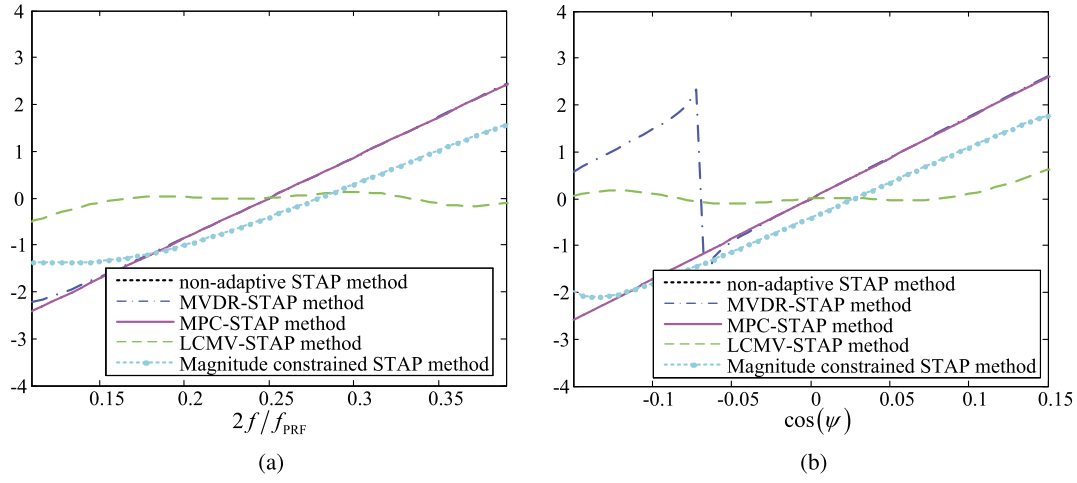

Fig. 4. Phase response curves in separated domain within the mainlobe region. (a) In temporal domain and (b) in spatial domain.

causing severe performance degradation. Fig. 7 shows the performance degradation of the proposed MPC-STAP around the clutter ridge. As it is clearly visible in this figure, the performance notch of the worst-case STAP method is much narrower than other techniques. The performance of MVDR-STAP method degrades due to target self-whitening and that of the LCMV-STAP method degrades dramatically because of the distorted mainlobe and high sidelobe. The proposed method outperforms other methods when the ve-

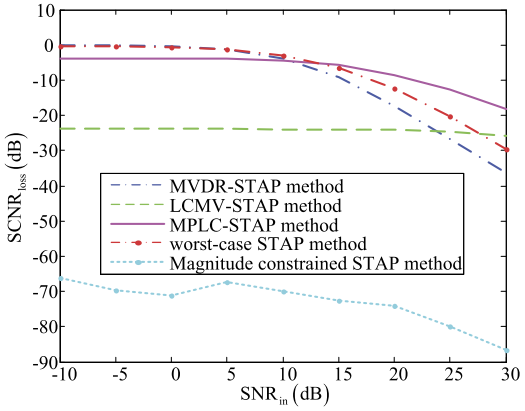

Fig. 5. SCNR loss versus input SNR.

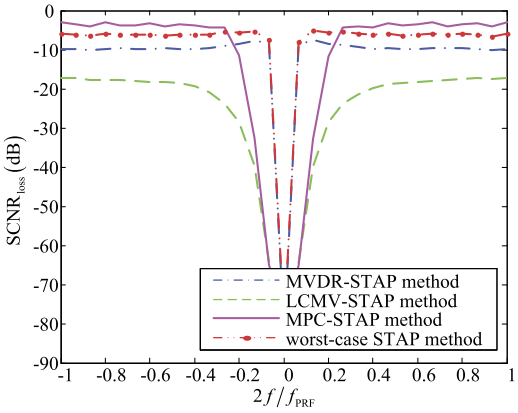

Fig. 7. SCNR loss versus Doppler frequency.

locity of the target is not too small. In practice, the Doppler bins which are very close to the clutter are excluded in the detection procedure to reduce the false alarm probability [28]. By increasing the number of coherent pulses, the performance notch of the proposed method can be narrow enough to meet the requirement in practice.

5. Conclusions

In this work, the phase constraint is incorporated in the response vector, resulting in the joint MPC-STAP approach. The proposed approach can be taken as an extended LCMV-STAP method with further exploration on the response vector. By exploiting the magnitude and phase constraints, the mainlobe of the STAP radar is well-maintained. Besides, the proposed method is robust against target contamination and improves the performance in terms of SCNR loss. Moreover, the conjugate symmetric characteristic of the adaptive weights is utilized to obtain the explicit expression of the phase constraint, which guarantees the distortionless response of STAP radar. Numerical simulations have verified that the proposed method is able to provide superior performance and robustness in target contamination situations.

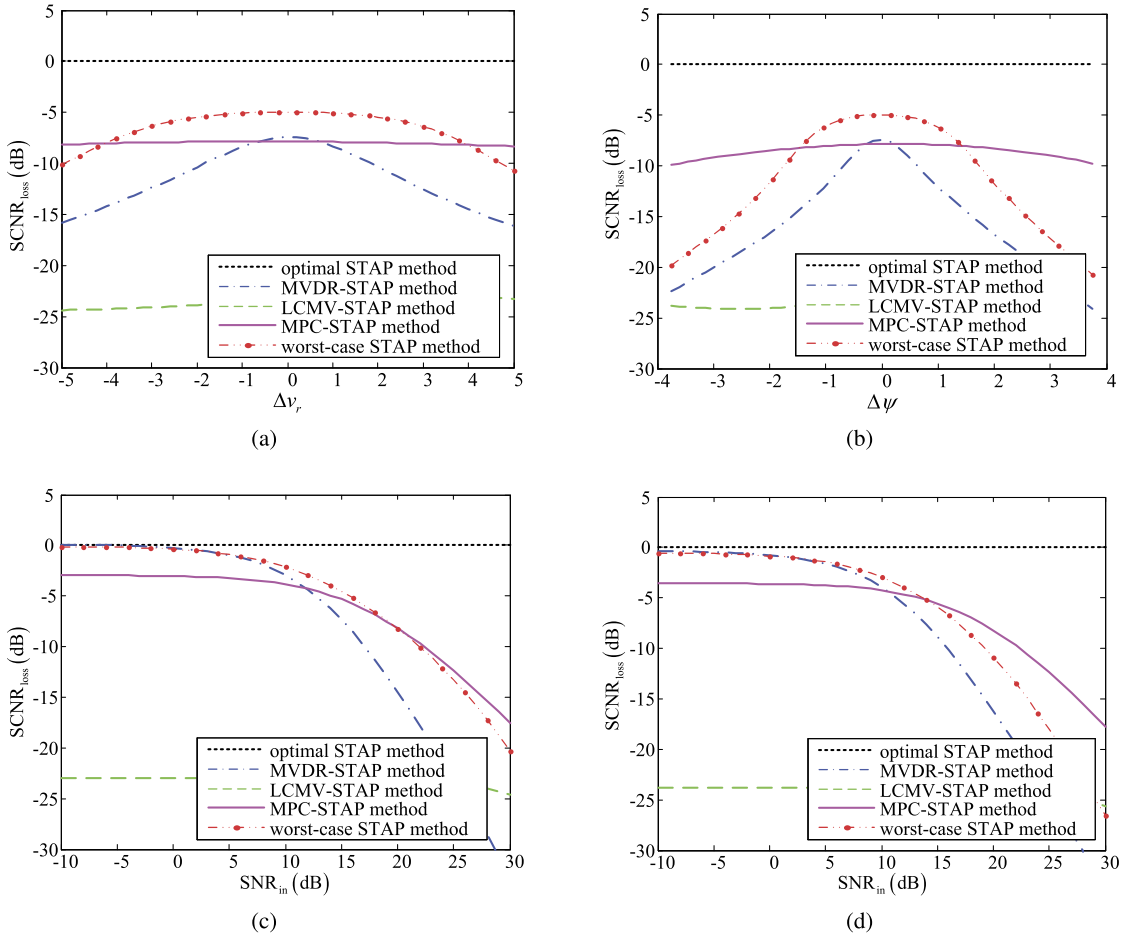

Fig. 6. SCNR loss in with mismatches in separated spatial or temporal domain. (a) SCNR loss performance versus velocity error, (b) SCNR loss performance versus angle error, (c) SCNR loss performance in spatial domain versus input SNR and (d) SCNR loss performance in temporal domain versus input SNR.

References

[1] J.R. Guerci, Space–Time Adaptive Processing, Artech House, Norwood, MA, 2003.
[2] S. Reed, J.D. Mallet, L.E. Brennan, Rapid convergence rate in adaptive arrays, IEEE Trans. Aerosp. Electron. Syst. 10 (6) (November 1974) 853–863.
[3] W.C. Xie, K.Q. Duan, F. Gao, Y.L. Wang, Z.H. Zhang, Clutter suppression for airborne phased radar with conformal arrays by least squares estimation, Signal Process. 91 (7) (July 2011) 1665–1669.
[4] H. Wang, L. Cai, On adaptive spatial-temporal processing for airborne surveillance radar systems, IEEE Trans. Aerosp. Electron. Syst. 30 (3) (July 1994) 660–670.
[5] J.R. Guerci, J.S. Goldstein, I.S. Reed, Optimal and reduced-rank STAP, IEEE Trans. Aerosp. Electron. Syst. 36 (2) (April 2000) 647–663.
[6] W.L. Melvin, M. Davis, Adaptive cancellation method for geometry-induced nonstationary bistatic clutter environments, IEEE Trans. Aerosp. Electron. Syst. 43 (2) (April 2007) 651–672.
[7] G. Borsari, Mitigating effects on STAP processing caused by an inclined array, in: IEEE National Radar Conference, Dallas, TX, May 12–13, 1998, pp. 135–140.
[8] B. Himed, Y. Zhang, A. Hajjari, STAP with angle-Doppler compensation for bistatic airborne radars, in: IEEE National Radar Conference, Long Beach, CA, May 22–25, 2002, pp. 22–25.
[9] P. Ries, F.D. Lapierre, J.G. Verly, Geometry-induced range-dependence compensation for bistatic STAP with conformal arrays, IEEE Trans. Aerosp. Electron. Syst. 47 (1) (January 2011) 275–294.
[10] S. Beau, S. Marcos, Range dependent clutter rejection using range-recursive space–time adaptive processing (STAP) algorithms, Signal Process. 90 (1) (January 2010) 57–68.
[11] M. Rangaswamy, F.C. Lin, K.R. Gerlach, Robust adaptive signal processing methods for heterogeneous radar clutter scenarios, Signal Process. 84 (9) (September 2004) 1653–1665.
[12] C.T. Capraro, G.T. Capraro, I. Bradaric, D.D. Weiner, M.C. Wicks, W.J. Baldygo, Implementing digital terrain data in knowledge-aided space–time adaptive processing, IEEE Trans. Aerosp. Electron. Syst. 42 (3) (July 2006) 1080–1099.
[13] B.D. Carlson, Covariance matrix estimation errors and diagonal loading in adaptive arrays, IEEE Trans. Aerosp. Electron. Syst. 24 (3) (July 1988) 397–401.
[14] R. Wu, Z. Bao, Y. Ma, Control of peak sidelobe level in adaptive arrays, IEEE Trans. Antennas Propag. 44 (10) (October 1996) 1341–1347.
[15] H. Cox, R.M. Zeskind, M.M. Owen, Robust adaptive beamforming, IEEE Trans. Acoust. Speech Signal Process. 35 (10) (October 1987) 1365–1376.
[16] J.L. Krolik, The performance of matched-field beamformers with Mediterranean vertical array data, IEEE Trans. Signal Process. 44 (10) (October 1996) 2605–2611.
[17] K. Takao, H. Fujita, T. Nishi, An adaptive array under directional constraint, IEEE Trans. Antennas Propag. AP-24 (5) (September 1976) 662–669.
[18] C.Y. Tseng, L.J. Griffiths, A unified approach to the design of linear constraints in minimum variance adaptive beamformers, IEEE Trans. Antennas Propag. 40 (12) (December 1992) 1533–1542.
[19] C.Y. Chen, P.P. Vaidyanathan, Quadratically constrained beamforming robust against direction-of-arrival mismatch, IEEE Trans. Signal Process. 55 (8) (August 2007) 4139–4150.
[20] J. Li, P. Stoica, Z. Wang, On robust Capon beamforming and diagonal loading, IEEE Trans. Signal Process. 51 (7) (July 2003) 1702–1715.
[21] S.A. Vorobyov, A.B. Gershman, Z.Q. Luo, Robust adaptive beamforming using worst-case performance optimization: a solution to the signal mismatch problem, IEEE Trans. Signal Process. 51 (2) (February 2003) 313–324.
[22] Z.L. Yu, W. Ser, M.H. Er, Z. Gu, Y. Li, Robust adaptive beamformers based on worst-case optimization and constraints on magnitude response, IEEE Trans. Signal Process. 57 (7) (July 2009) 2615–2628.
[23] Z.L. Yu, M.H. Er, W. Ser, A novel adaptive beamformer based on semidefinite programming (SDP) with magnitude response constraints, IEEE Trans. Antennas Propag. 56 (5) (May 2008) 1297–1307.
[24] B. Liao, K.M. Tsui, S.C. Chan, Robust beamforming with magnitude response constraints using iterative second-order cone programming, IEEE Trans. Antennas Propag. 59 (9) (September 2011) 3477–3482.
[25] J.W. Xu, G.S. Liao, S.Q. Zhu, Robust LCMV beamforming based on phase response constraint, Electron. Lett. 48 (20) (September 2012) 1304–1306.
[26] K.C. Huarng, C.C. Yeh, Adaptive beamforming with conjugate symmetric weights, IEEE Trans. Signal Process. 39 (7) (July 1991) 926–932.
[27] D. Xu, R. He, F. Shen, Robust beamforming with magnitude response constraints and conjugate symmetric constraint, IEEE Commun. Lett. 17 (3) (March 2013) 561–564.
[28] D. Cristallini, W. Burger, A robust direct data domain approach for STAP, IEEE Trans. Signal Process. 60 (3) (March 2012) 1283–1294.
[29] Z.C. Yang, X. Li, H.Q. Wang, W.D. Jiang, Adaptive clutter suppression based on iterative adaptive approach for airborne radar, Signal Process. 93 (12) (December 2013) 3567–3577.
[30] W.-S. Lu, A unified approach for the design of 2-D digital filters via semidefinite programming, IEEE Trans. Circuits Syst. I, Fundam. Theory Appl. 49 (6) (June 2002) 814–826.
[31] X. Lai, R. Zhao, On Chebyshev design of linear-phase FIR filters with frequency inequality constraints, IEEE Trans. Circuits Syst. II, Express Briefs 53 (2) (February 2006) 120–124.
[32] C.D. Meyer, Matrix Analysis and Applied Linear Algebra, SIAM, 2000.
[33] H.L. Van Trees, Optimum Array Processing (Detection, Estimation, and Modulation Theory, Part IV), Wiley, 2002.

Jingwei Xu received the B.S. degree in electrical engineering from Xidian University, Xi'an, China, in 2010. He is currently working toward the Ph.D. degree in the National Laboratory of Radar Signal Processing, Xidian University.

His research interests include space–time adaptive processing, robust adaptive beamforming, MIMO radar signal processing.

Zhengqi Zhu received the B.S. and Ph.D. degrees in electrical engineering from Xidian University, Xian, China, in 2005 and 2010, respectively.

In 2010 he joined Xidian University as a full assistant professor in National Laboratory of Radar Signal Processing where he was promoted to associate professor in 2012. In 2011 and 2014, he was awarded the Young Scientists Award for Excellence in Scientific Research by the International Union of Radio Science (URSI). Currently, he has been the reviewer for *IEEE Transactions on Aerospace and Electronic Systems, IEEE Transactions on Geoscience and Remote Sensing, Digital Signal Processing* and so on.

His research interests include space–time adaptive processing, multiple-input multiple-output radar, SAR ground moving target indication and sparse signal processing.

Guisheng Liao received the B.S. degree from Guangxi University, Guangxi, China, and the M.S. and Ph.D. degrees from Xidian University, Xi'an, China, in 1985, 1990, and 1992, respectively.

He is currently a Professor at the National Key Laboratory of Radar Signal Processing, Xidian University. He has been a Senior Visiting Scholar in the Chinese University of Hongkong, Hong Kong.

His research interests include space–time adaptive processing, array signal processing, SAR ground moving target indication, and distributed small satellite SAR system design. Dr. Liao is a member of the National Outstanding Person and the Cheung Kong Scholars in China.

Lei Huang received the B.Sc., M.Sc., and Ph.D. degrees in electronic engineering from Xidian University, Xian, China, in 2000, 2003, and 2005, respectively.

From 2005 to 2006, he was a Research Associate with the Department of Electrical and Computer Engineering, Duke University, Durham, NC. From 2009 to 2010, he was a Research Fellow with the Department of Electronic Engineering, City University of Hong Kong and a Research Associate with the Department of Electronic Engineering, The Chinese University of Hong Kong. From 2012 to 2014, he was a Full Professor with the Department of Electronic and Information Engineering, Harbin Institute of Technology Shenzhen Graduate School. Since November 2014, he has joined the College of Information Engineering, Shenzhen University, where he is currently a Chair Professor. His research interests include spectral estimation, array signal processing, statistical signal processing, and their applications in radar and wireless communication systems.

He is currently an associate editor of *IEEE Transactions on Signal Processing* and editorial board member of *Digital Signal Processing*.